Mansoura Engineering Journal (MEJ),Vol.18,No.1,March 1993. M. 11

# NATURAL CONVECTION IN VERTICAL AIR-FILLED ENCLOSURES - PART I

# الحمل الطبيعي في سياجات رأسية مملوءه هواء – جزء (١)

By
SHALABY, M.A.*, SHAHEEN, A.S.** and EL-SEDEEK, A**
(* Mech. Engg. Dept.,** Physical Science Dept.
Faculty of Engg., Mansoura University, Egypt.)

الخلاصة: يتضمن هذا البحث نتائج دراسة نظرية على الحمل الطبيعي داخل سياجات رأسية مملؤة هواء ، وذلك على إعتبار أن الجدران الرأسية للسياج عند حرارة ثابتة ، حيث أحد جدران السياج ساخن ، والجدار الآخر بارد والسريان في اتجاهين بعديين ، رقائقي ومستقر . ولقد نوقش تأثير النسبة الإعتبارية للسياج ( A وهي إرتفاع السياج مقسوم على عرضة ) على معامل الإنتقال الحراري والسريان بالحمل الطبيعي داخل السياج والدراسة النظرية تمت بإستخدام طريقة التحليل العددي لحل مجموعة معادلات ناڤيراستوك ومعادلة الطاقة في صورة المتغيرات الأصلية وذلك بإستخدام أكثر من نظام للفروق مثل CDS, UDS, HDS, PLS بهدف الوصول إلى نتائج دقيقة خلال زمن حسابي صغير كما ناقش البحث تأثير حجم الخلايا المقسم اليها حيز السياج على دقة النتائج . وخلال هذا البحث رقم ريليه تغير بين $١٠^{٣}$ إلى $١٠^{٦}$ ، والنسبة الإعتبارية أخذت القيمة من ١ إلى ١٠ ورقم براندل للهواء أخذ القيمة ٠,٧٣ . كما شمل البحث مقارنة بين النتائج التي حصلنا عليها والنتائج المتاحة عند الآخرين .

ABSTRACT - This study presents theoretical results on natural convection in vertical air-filled enclosures with isothermal hot and cold walls. The flow is considered to be two-dimensional laminar, and steady. The effect of the aspect ratio on the heat transfer and the natural convection flow is discussed. The effect of some finite difference schemes on the numerical method used has been discussed in this paper. The Rayleigh number varied from $10^3$ - $10^6$, the aspect ratio from 1-10 and the Prandtl number equals 0.73. A comparison has been also made with the available data in the literature.

## INTRODUCTION

Natural convection heat transfer in rectangular enclosures is of great importance in a number of engineering applications. The convective motion which results from buoyant effects arises, for example, in the insulation of a building, in the space between the absorber and cover plates of a solar collector, and in the gas-filled cavity surrounding a nuclear reactor core. In the enclosures, one vertical wall is usually considered to be at a high temperature and the other vertical wall at a low temperature. The horizontal surfaces of the enclosure are normally treated as adiabatic surfaces. Heat is transferred between the two vertical walls by conduction and / or convection. A vast majority of research in enclosures has been aimed at high aspect ratio (Large height to width ratio) enclosures perhaps because there are many applications of large aspect ratio enclosures. However, very few studies have been reported for enclosures of aspect ratio less than one, i.e. enclosures that are wider than they are high.

The natural convection problem in vertical enclosures has been investigated over a long period of time in the literature. Excellent reviews have been given by Ostrach [1] and Cotton [2]. Eckert and Carlson [3] and Elder [4] experiments show that different flow regimes can be distinguished : the conduction, the transition

and the boundary layer regime. In the boundary layer regime the upward and downward moving fluids are separated by a stratified core region. Though the stratification in the core region is very characteristic for natural convection in vertical enclosures, relatively little attention has been paid to its properties and its effect on the convective motion.

Schinkel, et.al. [5] studied theoretically natural convection in vertical air-filled enclosures with isothermal hot and cold walls. The flow was considered to be two-dimensional, laminar, and stationary. The effect of stratification of the fluid in the core region on the heat transfer and the natural convecting flow was discussed. The aspect ratio varied from 1-18, the Rayleigh number from $10^4$ - $10^6$ and the side walls were both perfectly conducting or adiabatic. They used in their solution the numerical method developed by Gosman, Pun and Spalding [6].

In the present study, we re-examined natural convection in vertical slots with special attention to the effect of the aspect ratio on the average heat transfer coefficient, as well as, the effect of the stratification in the core region. The flow is considered to be two-dimensional, laminar and stationary. The governing equations have been solved numerically using a semi-implicit method for pressure linked equations (SIMPLE) of finite differences suggested by Patankar [7]. The solution is provided with various differences scheme in order to obtain the more accurate results as well as to optimise the consumed time of solution.

## FORMULATION OF THE PROBLEM

A rectangular vertical slot as shown in Fig. (1) is considered. The two vertical walls have a uniform temperature, $T_h$ and $T_c$, respectively. $T_h$ is assumed to be higher them $T_c$. The distance between the vertical walls is L, and the height of the slot is H. The ratio H/L is called the aspect ratio, A. It is assumed that the problem can be considered as a two-dimensional one, i.e., the depth of the enclosure is assumed to be infinitly long. A cartesian coordinate system as shown in Fig. (1) is used.

The governing equations are the continuity equation, the Navier-Stokes equations and the energy equation. Following the well- known Obestreck-Boussinesq approximation [8] the dimensionless two-dimensional steady form of the governing equations can be written as,

$$\frac{\partial U}{\partial X} + \frac{\partial V}{\partial Y} = 0 \qquad (1)$$

$$U \frac{\partial U}{\partial X} + V \frac{\partial U}{\partial Y} = - \frac{\partial P}{\partial X} + \frac{\partial^2 U}{\partial X^2} + \frac{\partial^2 U}{\partial Y^2} \qquad (2)$$

$$U \frac{\partial V}{\partial X} + V \frac{\partial V}{\partial Y} = - \frac{\partial P}{\partial Y} + \frac{\partial^2 V}{\partial X^2} + \frac{\partial^2 V}{\partial Y^2} + \frac{g\beta H^3 (T_h - T_c)}{\nu^2} . \theta \qquad (3)$$

$$U \frac{\partial \theta}{\partial X} + V \frac{\partial \theta}{\partial Y} = - \frac{k}{\mu Cp} \left( \frac{\partial^2 \theta}{\partial X^2} + \frac{\partial^2 \theta}{\partial Y^2} \right) \qquad (4)$$

Various dimensionless groups appear above in the dimensionless equations (1-4), where H is the characteristic length, $g\beta H^3 (T_h-T_c) / \nu^2$ is called the Grashof number (Gr), $\mu$ Cp/k is called the Prandtl number (Pr) and $(T - T_c) / (T_h - T_c)$ is defined as the dimensionless temperature ($\theta$). The fluid properties are taken at the reference temperature, $T_o = (T_h + T_c) / 2$. Often the Rayleigh number (Ra) has been used where Ra = Gr. Pr. The equations (1-4) are known as the dimensionless equations in primitive variables form. These four partial differential equations have the unknown variables U, V, $\theta$ and P.

## THE GRID SPACING

The grid distribution in use is a uniform grid in the X and Y coordinates. The descrete location of interest on the X-co-ordinate, $X_i$ are spaced out uniformly and so are $Y_j$, with $\Delta X$ and $\Delta Y$ as their respective increments, Thus,

$$X_{i+1} = X_i + \Delta X \tag{5}$$

$$Y_{j+1} = Y_j + \Delta Y \tag{6}$$

Fig. (2) shows the position of the variables $\theta$, U, V and P. The scalar variables pressure (P) and temperature ($\theta$) are defined on the scalar nodes $(X_i, Y_j)$, while this is not true for the velocity components U and V. The U velocity is defined half way between two scalar nodes on the Y-line and the V velocity is defined halfway between two scolar nodes on the X-line. This means that, $U_{i,j}$ is defined at $(X_i + \frac{\Delta X}{2}, Y_j)$ and $V_{ij}$ is defined at $(X_i, Y_j + \frac{\Delta Y}{2})$ because the fractional subscripts are not used.

## STABILITY CONDITION

The descretisation in domain has a general form of the finite-difference equation which is represented as

$$A_P \phi_P + A_W \phi_W + A_E \phi_E + A_N \phi_N + A_S \phi_S = R_P \tag{7}$$

The variable $\phi$ may represent a component of velocity, pressure or temperature and is related to its neighbours on finite difference grid. The point P has four neighbours which may be represented by N,S,E and W. In equation (7), $A_P, A_N, A_S, A_E$ and $A_W$ are functions of the grid size and medium properties. The convergence and stability of these procedures require that the coefficientsof equation (7) satisfy the following conditions:

$$A_P \geq 0 \tag{8}$$

$$A_E, A_W, A_N, A_S \leq 0 \tag{9}$$

$$A_P \geq |A_E| + |A_W| + |A_N| + |A_S| \tag{10}$$

## BOUNDARY CONDITIONS

The boundary conditions of the specified problem are:

Top wall : $Y = 1$ $U = 0,\ V = 0,\ \frac{\partial \theta}{\partial Y} = 0$ (11)

Bottom wall; $Y = 0$ $U = 0,\ V = 0,\ \frac{\partial \theta}{\partial Y} = 0$ (12)

Left side; $X = 0$ $U = 0,\ V = 0,\ \theta = 1$ (13)

Right side; $X = A$ $U = 0,\ V = 0,\ \theta = 0$ (14)

## DIFFERENCE SCHEME

During the scope of this work, the obtained expressions used the central difference scheme (CDS), the upwind difference scheme (UDS), The hybrid difference scheme (HDS) and the power-law difference scheme (PLS). The equations (1 - 4) are in the so-called hydrodynamical form. We used the SIMPLE method developed by Patankar [7] to solve the equations ( 1- 4 ). The method is based on the method of finite difference and is described in detail in [9].

The ADI method is considered which uses line by line procedure in two directions alternately introduced by Peaceman and Rachfold [10]. Consider the finite difference equation (7), the ADI procedure computes $\phi^1$ from $\phi^0$ in two steps. It is noted that the explicit scheme in Y-direction and the implicit scheme in X-direction which requires only tridiagonal system solution. And then, the explicit scheme in X-direction and the implicit scheme in Y-direction which again requires only tridiagonal system solution so the set of finite difference equations are iteratively solved by the ADI method. In each iteration the energy equation is solved first to obtain the temperature distribution at each nodal point, in the cavity domain. Using these values, the momentum equations are solved to obtain the velocity and pressure distributions. The procedure is repeated till the required convergence is obtained.

## CONVERGENCE CRITERIA

The quantitative criteria to terminate the calculations are determined as comparison between the attained accuracy and the amount of computation time required. In the cavity, convergence criterion is individually applied to all the four variables $\theta$, U,V and P. The convergence criterion used is:

$$\left| (\phi^{m+1} - \phi^{m}) / \phi^{m} \right| \le \varepsilon \qquad (15)$$

where $\phi$ is the unknown variable and m indicates the iteration number and $\varepsilon$ is the chosen accuracy, during the course of this work, the value of $\varepsilon$ is in between $0.1 \times 10^{-3}$ and $5.0 \times 10^{-5}$.

## VALIDITY OF THE NUMERICAL SCHEME

The comparison of convective heat transfer in cavities often takes different shapes, depending on the conditions of buildings. A large amount of work has been done on the square cavity problems (see the report made by Davis and Jones [11]), so the validity of the numerical scheme can be checked by the comparison of the present results on the square cavity with the same obtained in the available literature review. Attempts are made to obtain solution of the square cavity using the hybrid difference scheme (HDS) and power law scheme (PLS).The present results are in excellent agreement with bench mark solution of Davis [13]. It is also found that the power law scheme reduces the number of iterations as shown in Table (1). The table also shows that the number of iterations decreases more by using false transient [12] with the power-law scheme. So, the last mentioned scheme has been chosen to be used in the numerical solution of the different shapes of the cavities included in this paper, as well as in the next work.

During the course of the present work, we have special attention in the steady state solution of the problem. Therefore, the foregoing procedures are inefficient, however, the solution may be obtained more efficiently by adding the false transient term to the governing equations. The false transient term leads to a set parabolic equations which are solved by marching through a distorted time. The true transient time is lost, but with the transient terms decay and the true steady state solution is recovered.

## RESULTS AND DISCUSSION

As mentioned above the test problem for the numerical method, the grid size and the difference schme, is the case for A = 1. In Fig. (3), Nu is shown as a function of Ra and the present results are in excellent agreement with Shalaby et. al. [14] and Davis [13], who used high accurate methods. The present values of Nu are correlated by the least square as follows:

$$Nu = 0.142\ Ra^{0.302} \qquad 10^3 \le Ra \le 10^7, \quad A = 1 \qquad (16)$$

where $Ra = Gr.Pr$, $Pr = 0.73$ for air.

For other aspect ratios, the correlations for average Nusselt numbers are derived in the general form:

$$Nu = a.\ Ra^{b} \qquad (17)$$

where a and b are constants varied with the different values of the apsect ratios. Table (2) shows the constants a and b of the correlation (17) for the case of $A \ge 1$. These correlations fit the present numerical results with 0.5% as shown in Fig. (4), for $10^3 \le Ra \le 10^6$. One may observe that, the Nu value decreases for example, at $Ra = 10^6$ and $A = 4/3$, $Nu = 9.02$ and as the aspect ratio increases, if A =10 the Nu value equal to 7.3. It is also seen that the differences between the Nu values for each aspect ratio with respect to the same for the other aspect ratios decreases with the increase of Ra value.

## VELOCITY PROFILES

From the governing equations and the boundary conditions, one may observe that the situation is symmetric around the centre of the cavity, i.e. at

X = 0.5 A and Y = 0.5. Therefore, the velocity profiles along each half of the cavity are drawn in Fig (5). The figures show the vertical velocity component V at the midheight of the cavity (Y = 0.5), for Ra = $10^4$, $10^5$ and $10^6$ at A = 1, 4/3 and 2. One may observe that the reverse flow occurs near the cavity centre at A = 1 and 4/3 for Ra = $10^5$ and $10^6$, but this phenomenon disappears with the increase of the aspect ratio. It is also observed that the velocity components are very close to zero at the cavity core region, hence the heat is transferred across the core region by conduction. As Ra increases the boundary layer thickness becomes thinner and the Nu values increase. It is also observed that, as the aspect ratio increases. the V velocity component decreases comparatively for the same values of Ra. As a result of the above observations, one may conclude that the veritcal slots become a good insulation as expected as A increased.

## FLOW REGIMES

Different criteria can be used, in order to define the starting of the boundary layer regime. Eckert and Carlson [3] considered the horizontal temperature gradient at the central point $(\partial\theta / \partial X)_0$ of the cavity. The starting of the boundary layer regime then is defined as (Ra, A) combination where this gradient becomes zero for the first time. On the other side, Gill [15] considered the shear stress at the central point $(\partial V / \partial X)_0$. This is used as criterian that (Ra, A) combination where this stress becomes zero. From our calculations it is observed that the horizontal isothermal lines start to occure at the core of the enclosure when Ra has a value between $10^3$ and $10^4$, in the case of square cavity [9] and this show that our results are in quite good agreement with the same obtained by Eckert and Carlson.

Fig. (6-left) shows that the constant temperature lines ( the isothermal lines)for Ra = $10^5$ and at A = 4/3, 4 and 10. These lines are plotted in uniformal increments euqual to 0.1. In Fig. (6-a) at A = 4/3 the isothermal lines are veritcal at the ends of the walls and are parallel to the vertical sides. These lines are concentrated at the starting ends of the boundary layer in which the local heat transfer coefficients are higher than the corresponding values at the departure corners of the boundary layer. At the center of the cavity the isotherms are horizontal with a slight positive slope. This positive slope in the core region shows that, the flow of heat transfer by conduction, in the central portion of the cavity is against the overall direction of the heat transfer flow. One may also observe that, the isotherms of Fig (6-a and b) clearly show the stratification of the core region. The temperature in the vertical direction in the core region depends almost linearly on Y and the temperature gradient in vertical direction is positive. It is also observed that as the aspect ratio increases from 4/3 to 4, the isotherms in the domain of the enclosure changes to become more vertical. And in Fig (6-c) the isotherms become almost vertical, this proves that the flow of heat by conduction increases with the aspect ratio (A) to be the main mode of heat transfer at A = 10.

Fig (6 -right) also shows the contour maps of stream lines for A = 4/3, 4 and 10 at Ra = $10^5$. The stream lines are plottted in uniform increments ot $\Delta\Psi$ which is different for each aspect ratio. The used symbols in graphics, indicate the strength of circulation in the stream lines domain. In Fig. (6-a-right) for A = 4/3, and at Ra = $10^5$, it is seen that there are two eddies near the center of the cavity and the incremental $\Delta\Psi$= 0.7 and the maximum strength of streamlines is 13.6. One may also observe some secondary flow exists at the corner regions as well as it appears near the side walls.

In Fig. (6-b) for aspect ratio A = 4 it is seen that, the stream lins have a single eddy at the center of the cavity domain. The maximum value of stream lines strength are 5.5 for Ra = $10^5$. As the aspect ratio increases to be equal to 10. (see Fig. 6-c), one may observe that, beside the vortex at the cavity center,

there are three eddies appear at each of the boundary layer departure corner. This type of the secondary motion occurs at high aspect ratio A = 10, and causes a tertiary motion located between the secondary motion described above. The secondary motion has the same rotation as the primary motion, while the tertiary motion rotates in the opposite direction.

## COMPARISON WITH AVAILABLE DATA

The results obtained in the present work are plotted in Figures (7 and 8) for A = 2 and 10 in comparison with the same obtained by Schinkel et.al. [5] and Markatos [16]. The Figure shows the variation of the average Nusselt number (Nu) versus Rayleigh number. It is seen that the present results are in quite good agreement with the same obtained by Schinkel et.al. [5] for A equal to 2 and 10, while the agreement is comparatively good with Markatos for A equal to 2.

## CONCLUSIONS

Out of the present work one may conclude that:

1. The rate of heat transfer through the vertical enclosure decreases with the increase of the aspect ratio.

2. As the aspect ratio of the vertical slot increases, at a certain Rayleigh number value, the number of eddies also increases and may take the elliptic shape along the vertical axis.

3. The boundary layers, along the hot and the cold walls of the cavity, interface with the increases of the aspect ratio, i.e. the heat transfer coefficient decreases.

4. The circulation strength and the secondary flow increase with the Rayleigh number increase and the tertiary flow may appear at high values of Ra and A.

## NOMENCLATURE

| | |
|---|---|
| A | aspect ratio (H/L) from 1 to 10,finite difference coefficient, |
| a,b | correlation constants, |
| Cp | specific heat, |
| g | acceleration of gravity, |
| Gr | Grashof number ($g \beta \Delta T H^3/\nu^2$), |
| H | cavity height, |
| h | heat transfer coefficient, |
| k | thermal conductivity of fluid, |
| L | cavity width, |
| $l_0$ | scale for length, |
| Nu | average Nusselt number, (hH/k), |
| Ra | Rayleigh number (Gr.Pr), |
| P | dimensionless pressure $p / (\rho u_0^2)$, |
| p | pressure, |

| | |
|---|---|
| Pr | Prandtl number ( $\mu$ Cp/k), |
| T | temperature, |
| $T_0$ | reference temperature, |
| t | time, |
| U,V | component of dimensionless velocity in X and Y ,direction respectively $(\frac{u}{u_0}, \frac{v}{u_0})$, |
| $u_0$ | scale for velocity, $(\nu / l_0)$, |
| X, Y | dimensionless distances in x and y cartesian coordinates, $(\frac{x}{l_0}, \frac{y}{l_0})$, |
| $\Delta X, \Delta Y$ | dimensionless mesh sizes in x and y cartesian coordinates |

**Greek Letters**

| | |
|---|---|
| ß | volumetric expansion, (1/K), |
| $\theta$ | dimensionless temeprature, $(T-T_0)/\Delta T$, |
| ø | dummy variable |
| $\rho$ | fluid density, |
| $\mu$ | dynamic viscosity |
| $\nu$ | kinematic viscosity, |
| $\psi$ | stream function |

Subscripts

| | |
|---|---|
| c | cold side, |
| h | hot side,, |
| P | nodal point |
| E | east, |
| W | west, |
| N | north, |
| S | south. |

REFERENCES


1. Ostrach, S., "Natural Convection in Enclosures", Advances in Heat Transfer, Vol.8, pp. 161-227, (1972).

2. Catton, I., "Natural Convection in Enclosures", Proceedings of the Sixth International Heat Transfer Conference, Toronto Canada, vol. 6, pp. 13-31 Aug. 7-11, (1978).

3. Eckert, E.R.G., and Carlson, W.O., "Natural Convection in an Air-layer Enclosed Between Two Vertical Plates With Different Temperatures", International Journal of Heat and Mass Transfer, vol.2, pp. 106-120, (1961).

4. Elder, J.W., "Laminar Free Convection in a Vertical slot", Journal of Fluid Mechanics vol. 23, pt. 1, pp. 77-98, (1965).

5. Schinkel, W.M.M., Linthorst, S.J.M. and Hoogendoorn, C.J, " The Stratification in Natural Convection in Vertical Enclosures"., Journal of Heat Transfer, vol. 105, pp. 267-272, May (1983).

6. Gosmen, A.D., Pun, W.M. and Spalding, D.B., "Lecture Note for Course Entited Calculations of Recirculating Flows, "Imperial College of Science and Technology, London, (1973).

7. Patankar, S.V , "Numerical Heat Transfer and Fluid Flow", McGraw Hill New York (1980).

8. Boussinesq, J., "Theorie Analytique de chaleur", Vol. II, p. 172. (1954).

9. Shaheen, A.S.A., "Numerical Solution of The Natural convection Heat Transfer Problems", M.Sc., Thesis, Mansoura University, Egypt (1989).

10. Peaceman, D.W. and Rachford, H.H., " The Numerical Solution of Parabolic and Elliptic Differential Equation". J.Appl. Math. Vol.1, pp 28-42, (1955).

11. Davis, D.G. and Jones, I.P., "Natural Convection in a Square Cavity a Comparison Exercise", Report A.E.R.E., Harwell, U.K., (1981).

12. Mallinson. G.D. and De Vahl Davis, "The Method of the False Transient for the Solution of Coupled Elliptic Equations", J. Computation Physics, (1973).

13. De Vahl Davis, G., "Laminar Natural Covection in an Enclosed Rectangular Cavity", International Journal of Heat and Mass Transfer, Vol. 11., pp. 1675-1693. (1968).

14. Shalaby, M.A., Gaitonde, U.N, and Sukhatme, S.P. "Laminar Natural Convection in an Enclosed square cavity", J.Thermal Engineering, Vol.3, pp. 72-82, (1983).

15. Gill, A.E., "The Boundary-Layer Regime for Convection in a Rectangular Cavity". Jr. of Fluid Mech. Vol. 26, pt. 33, pp. (515-536), (1966).

16. Markatos, N.C. and Pericleous, K.A., "Laminar and Turbulent Natural Convection in an Enclosed Cavity", Int. Jr. Heat Transfer, Vol. 27 pp. (755-772), (1984).

Table (1) The Variation of Iteration Numbers With Different Schemes

| SCHEME TYPE | 18 X 18 Grids | | | 34 X 34 Grids | | |
|---|---|---|---|---|---|---|
| | $R_a=10^4$ | $10^5$ | $10^6$ | $10^4$ | $10^5$ | $10^6$ |
| Hybrid scheme | 34 | 39 | 43 | 50 | 80 | 88 |
| Power law scheme | 30 | 36 | 41 | 34 | 47 | 66 |
| Power law with false | 18 | 19 | 35 | 22 | 28 | 48 |
| - Transient (dt)* | (0.04) | (0.008) | (0.002) | (0.04) | (0.01) | (0.002) |

* The values between paranthese represent the false-transient parameters

Table (2) The Correlation Constant a and b for $A \geq 1$

| A | a | b |
|---|---|---|
| 1 | 0.142 | 0.302 |
| 4/3 | 0.1222 | 0.3028 |
| 2 | 0.1222 | 0.3090 |
| 4 | 0.0853 | 0.3304 |
| 10 | 0.0253 | 0.4098 |

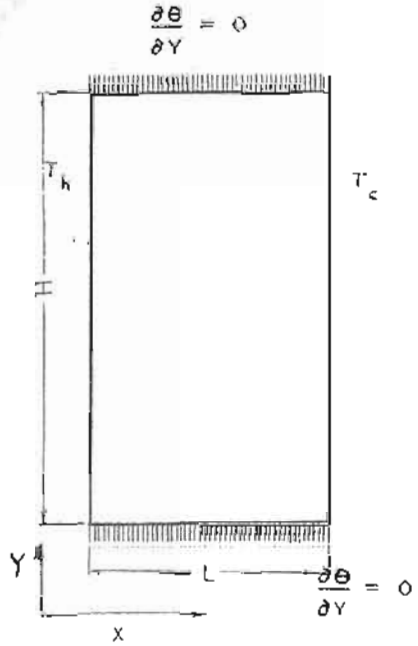


Fig. (1) Geometry of Vertical Cavity

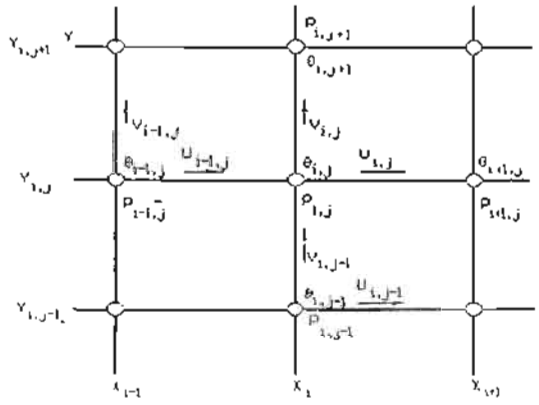

Fig. (2) Straggered Grids for $U_{ij}$ and $V_{ij}$

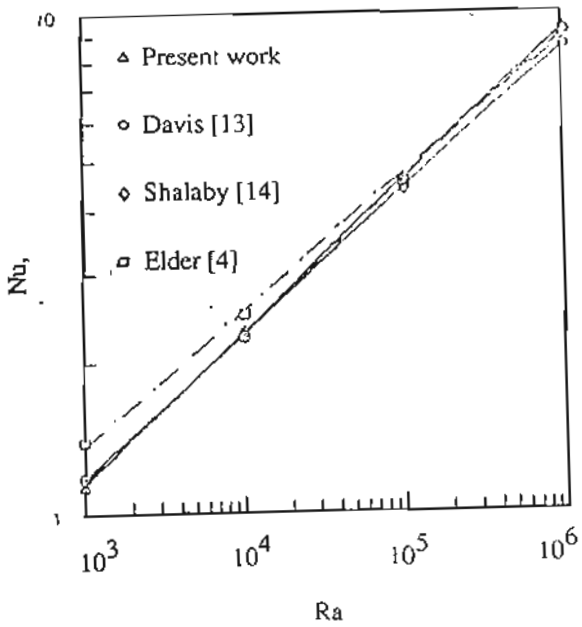


Fig. (3) Nusselt Number Versus Rayleigh Number as a Comparison with other References

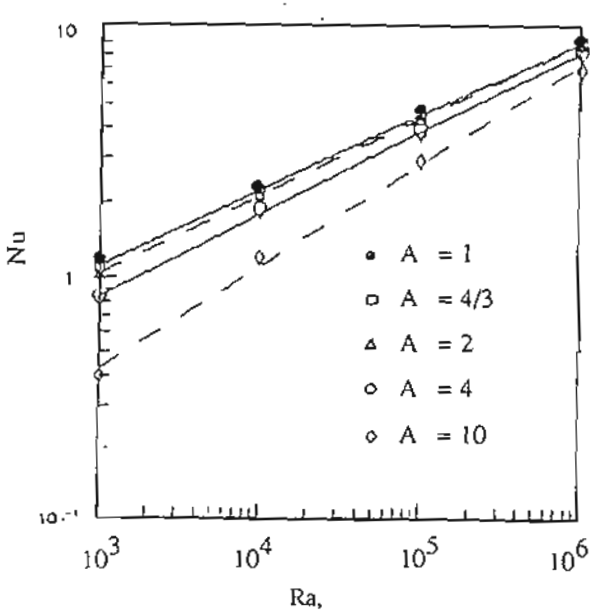


Fig. (4) Nussel Number Versus Rayleigh Number at Different Aspect Ratios

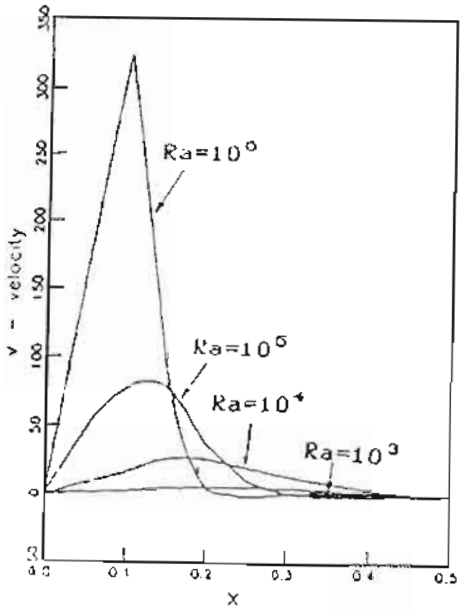


(a) A = 1

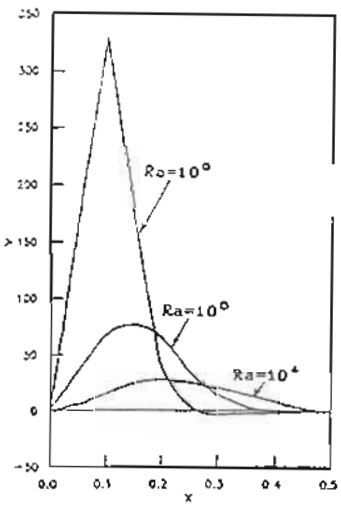


(b) A = 4/3

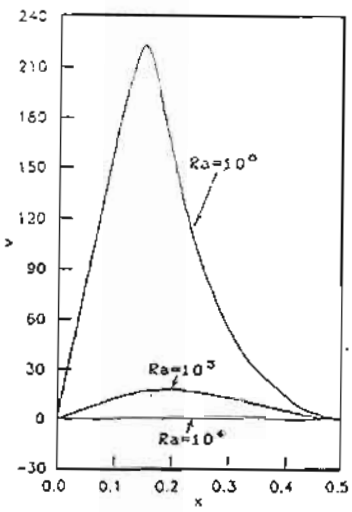


(c) A = 2

Fig. (5) Vertical Velocity Component at Midheight of the Cavity with Different Aspect Ratios
(a) A =1, (b) A = 4/3 and (c) A = 2.

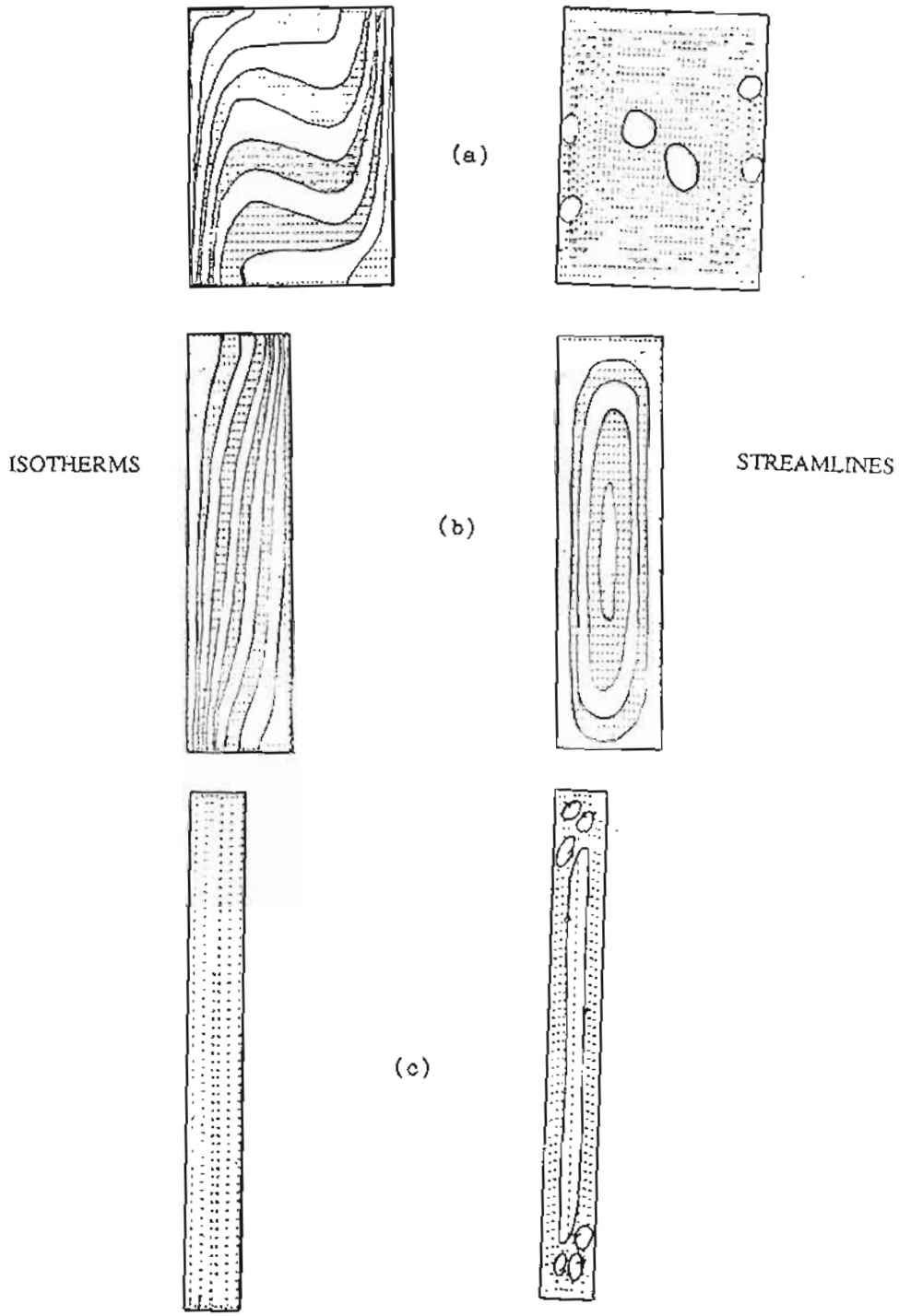


Fig. (6) Some Typical Examples of Isotherms (left) and Streamlines (Right) at $Ra = 10^5$ for (a) 4/3, (b) A = 4 and (c) A = 10

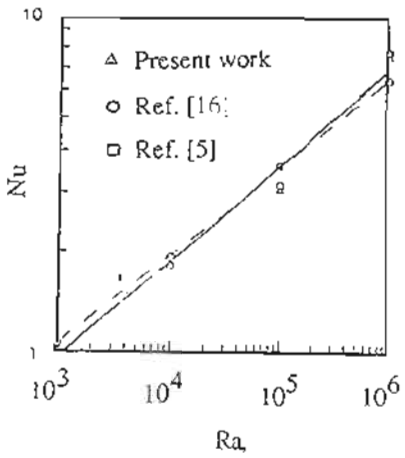


Fig. (7) Comparison of Nusselt Number Results With The Data of Schinkel [5] Markatos [16] for A = 2

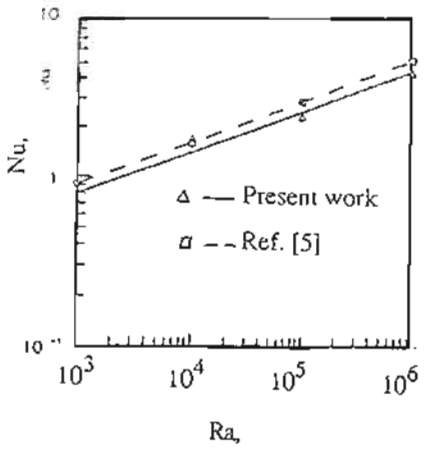


Fig. (8) Comparison of Nusselt Number Results With the Data of Schinkel [5] for A = 10